Eur. Phys. J. B **8**, 497–505 (1999)

THE EUROPEAN PHYSICAL JOURNAL B

EDP Sciences

Electronic and magnetic structure of the undoped two and three-leg ladder cuprates in an itinerant electrons model

Ph. Germain[1,2,a] and M. Laguës[1]

[1] Laboratoire Surfaces et Supraconducteurs, École Supérieure de Physique et Chimie Industrielles de la ville de Paris, 10 rue Vauquelin, 75231 Paris Cedex 5, France

[2] Groupe de Physique des Milieux Denses, UFR Sciences - Université Paris XII, 61 avenue du Général de Gaulle, 94010 Créteil Cedex, France

Received 3 June 1998

Abstract. We study the electronic and magnetic structure of the undoped ideal two and three-leg ladder cuprates by assuming a moderate *on site* coulombic repulsion. This analysis is an extension of the Fermi liquids studies proposed for the CuO_2 plane in view to explain the high T_c superconductivity and the competition with the antiferromagnetic phase. At zero doping, the quasi-one-dimensionality of the structure results in SDW correlations with different (commensurate) vectors according to the number of legs, which contrasts with the predictions made from the Heisenberg model. At mean field, and for $n = 3$ ($Sr_2Cu_3O_5$), we predict a magnetic ordered state, detected by μSr and NMR measurements with critical temperatures consistent with our assumptions on the physical parameters, the modulation vector being $\pi/2$. The presence of several bands at the Fermi level explains why there is no observable gap in the static susceptibility measurements. For $n = 2$, we predict a gap consistent with experimental Curie susceptibility. But the expected magnetic instability is detected only in $La_2Cu_2O_5$, where the interladder coupling is stronger. In every case the one-dimensional van Hove singularities are far from the Fermi level, making difficult the obtaining of high T_c superconductivity.

PACS. 74.70.-b Superconducting materials (excluding high-T_c compounds) – 74.20.-Fg Superconducting materials (excluding high-T_c compounds) – 75.10.-Lp Band and itinerant models

1 Introduction

It is a common idea that the superconductivity in the cuprates cannot be understood independently of their magnetic properties: indeed spin fluctuations are observed even in the superconducting phase, and a gap in the spectrum of the spin excitations is evidenced in inelastic scattering neutron measurements [1]. This has been identified as the *spin gap* of the strong interactions t-J model [2], according to which it would stabilize the superconducting holes pairs in the doped CuO_2 plane [3]. On the other hand, sizeable isotope effects on the critical superconducting temperature [4], but also charge ordering involving the crystal lattice [5] and competing the superconductivity [6], have been observed in many compounds, raising the influence of the electron-phonon coupling on pairing. It is therefore an extremely controversial question as to whether superconductivity finds its physical origin in the spin correlations, or simply coexists with them, the pairing being due to another mechanism, such as the electron-phonon interaction.

To clarify this question the symmetry of the gap has been intensively studied, since this latter is closely related to the pairing mechanism [7]. Alternatively, the discovery of a new class of cuprates, the ladder compounds [8], has opened a new track of investigations. These systems consist of n parallel Cu–O chains interacting through Cu–O–Cu bounds. Typical examples are the $SrCu_2O_3$ ($n = 2$) and $Sr_2Cu_3O_5$ ($n = 3$) compounds, where the structure induces a very weak interladder coupling [8]. Up to now, they have been considered essentially as Mott insulators, and described in the limit of strong local repulsion, with an antiferromagnetic Heisenberg model [9]. The most striking result in this limit is that the nature of the ground state and the excitations spectrum are critically different whether the number of legs of the ladder is even or odd: roughly, the two-leg ladder can be regarded as made of singlet pairs $S = 0$ stabilized along each rung by the AF coupling, whereas in the three-leg ladder the fundamental of each rung has a total spin $S = 1/2$. The former is therefore expected to be magnetically disordered, with a spin gap corresponding to triplet excitations observable in susceptibility and NMR measurements. On the contrary, the latter has gapless collective modes and may exhibit an AF long range order stabilized by the presence

[a] e-mail: germain@univ-paris12.fr

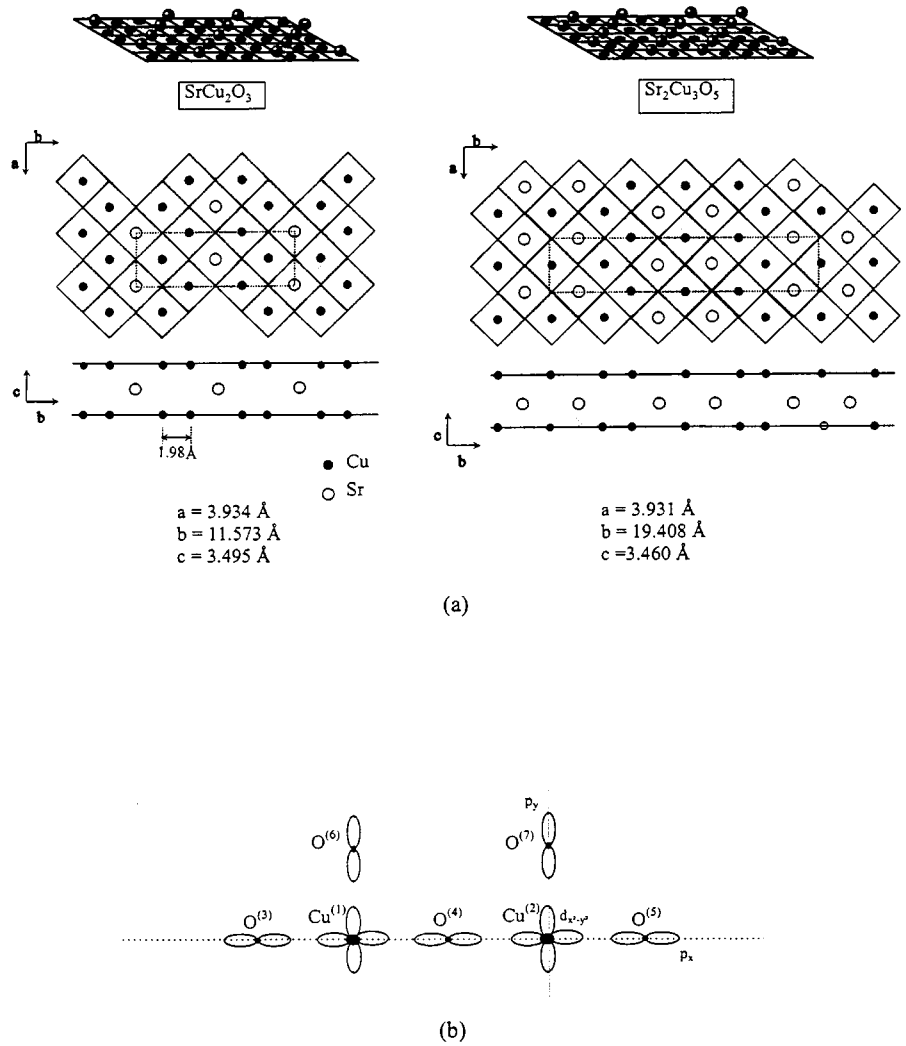

Fig. 1. (a) Structure of the plane $Cu_nO_{2_{n-1}}$ for $n = 2$ ($SrCu_2O_3$) and $n = 3$ ($Sr_2Cu_3O_5$) [8]. (b) Unit cell of the two legs ladder.

of a weak 3D coupling. Various numerical studies [10,11] confirm this picture, which strongly privileges the coupling along each rung, even in the *true* physical case where the perpendicular coupling along the legs has the same magnitude as along the rungs (one finds $\Delta^{spin\ gap} = J/2$ for the two-leg ladder [9–11]). In the two-leg ladder this results in superconducting or CDW correlations between singlet holes pairs upon doping [10,12].

The scenario is quite different if we study these systems on the other side of the Mott transition, *e.g.* for a coulombic repulsion smaller than the bandwith ($U < W$): starting from the weak coupling limit, the ladder has a quasi 1D band structure, with a nested Fermi surface, leading to spin density waves correlations for different wave vectors according to the number of legs: for instance, for $n = 2$, the nesting vector is $q = 2\pi/3$ along the direction of the ladder [13], whereas for $n = 3$, we find in this paper the two vectors $q_1 = \pi/2$ and $q_2 = \pi$. The interladder coupling should also play an important role since an AF state has been found to be stable [14] in the weak coupling regime, for the specific case of $La_2Cu_2O_5(n = 2)$ where the interladder coupling is much stronger than in $SrCu_2O_3$. Moreover, in a standard electron-phonon mechanism these correlations are expected to compete with the superconductivity by opening a gap at the Fermi level. Therefore, a part from its intrinsic interest, and the search of new superconductors, the ladder compounds should provide excellent tests for the validity of the theories and the understanding of the high T_c mechanism.

The superconducting copper oxides are mostly considered as strongly interacting systems on the basis of the high energy photoemission spectroscopy (UPS, XPS) that shows the existence of satellites attributed to the local on site repulsion on the copper atoms [15]. However these results do not constitute a direct measurement of U, and weak coupling approaches have also been proposed to describe the electronic and magnetic structure of the CuO_2 plane. These could explain many of their physical properties, by introducing a standard BCS coupling and moderate coulombic repulsion: high T_c superconductivity

$$\begin{bmatrix} \varepsilon_d & 0 & -\gamma'_x & \gamma_x & 0 & \gamma_y(1-\mathrm{e}^{-ika}) & 0 \\ 0 & \varepsilon_d & 0 & -\gamma_x & \gamma'_x & 0 & \gamma_y(1-\mathrm{e}^{-ika}) \\ -\gamma'_x & 0 & \varepsilon_p & 0 & 0 & 0 & 0 \\ \gamma_x & -\gamma_x & 0 & \varepsilon_p & 0 & 0 & 0 \\ 0 & \gamma'_x & 0 & 0 & \varepsilon_p & 0 & 0 \\ \gamma_y(1-\mathrm{e}^{ika}) & 0 & 0 & 0 & 0 & \varepsilon_p & 0 \\ 0 & \gamma_y(1-\mathrm{e}^{ika}) & 0 & 0 & 0 & 0 & \varepsilon_p \end{bmatrix} \begin{bmatrix} a_{n,k} \\ b_{n,k} \\ c_{n,k} \\ d_{n,k} \\ e_{n,k} \\ f_{n,k} \\ g_{n,k} \end{bmatrix} = \varepsilon_{n,k} \begin{bmatrix} a_{n,k} \\ b_{n,k} \\ c_{n,k} \\ d_{n,k} \\ e_{n,k} \\ f_{n,k} \\ g_{n,k} \end{bmatrix} \tag{1b}$$

due to the (experimentally observed) van Hove singularity, anomalous isotope effect [16,17] and gap anisotropy [18], and competition between antiferromagnetism and superconductivity according to the doping [19,20]. The correct description of the strange metal state (Fermi Liquid *vs.* non Fermi Liquid) is also controversial. From a Fermi Liquid point of view, there exists various proposals to describe the anomalous properties of the metallic phase by the nearness of the magnetic instability (in a weak [19,21,22], but also strong coupling scheme [23]), or, alternatively, by the proximity of the van Hove singularity [24], or charge instability in the presence of strong correlations [25]. These questions are intensively studied, one question being to describe in a consistent way the system close to the instability by diagrammatic expansions. In this context, extending the limit $U < W$ to the ladder cuprates should also be instructive, as the strong coupling limit is already being investigated.

A magnetic susceptibility measurement performed in $SrCu_2O_3$ [26] has confirmed the prediction of the existence of a gap in the two-leg ladder, since this susceptibility could be fitted by the law $\chi(T) \propto T^{-1/2} \exp(-\frac{\Delta}{T})$expected from the Heisenberg model [27], with $\Delta = 420$ K. This gap seems to be absent in $Sr_2Cu_3O_5$, in agreement with the *spin gap* scenario. Moreover, NMR and μSR experiments [28,29] indicate the existence of a long range order in $Sr_2Cu_3O_5$ (with $T_c = 55$ K). However, the *spin gap* found in NMR for $SrCu_2O_3$ is $\Delta' = 680$ K [30], much larger than Δ. Moreover, a magnetic transition has been observed in the $n = 2$ compound $La_2Cu_2O_5$ with $T_c = 117$ K [31] although the magnetic susceptibility measurements had found previously that $\chi(T)$ was remarkably similar to the one of $SrCu_2O_3$, with $\Delta = 473$ K [32] (see Sect. 3.1).

As progress are made in the synthesis of the ladders materials, the experimental situation will be progressively clarified. That is why we propose to study in this paper the alternative theoretical scenario of an itinerant electrons model [13]. In Section 2 we calculate analytically a simplified band structure for an isolated two-leg and three-leg ladder. We show that their quasi-one-dimensional character induces nesting instabilities of the Fermi surface. In Section 3, we treat the resulting magnetic instabilities in the mean field approximation, and discuss the experimental results. We point out the qualitative differences expected in comparison with the strong interactions limit. Section 4 is the conclusion.

2 Band structure of the ladders

2.1 The two-leg ladder

The ladder plane Cu_2O_3 of $SrCu_2O_3$ is shown in Figure 1a: each ladder is made of two Cu-O(I) chains coupled by Cu-O(II)-Cu rungs. Two adjacent ladders are structurally linked by Cu-O(II) bounds, parallel to the **b** vector. The unit cell, containing ten atoms (Cu_4O_6), is tripled along **b**, with $b = 3a$ ($a = 3.934$ Å, $b = 11.573$ Å and $c = 3.495$ Å [8]). In the Cu_2O_3 plane, each copper atom is surrounded with four oxygen neighbors, as in the standard CuO_2 plane. The difference comes from the fact that each O(I) atom is coupled to the copper atoms of the two adjacent ladders by two different respective orbitals: p_x and its orthogonal p_y. By neglecting their small coupling induced by the crystal lattice, the electronic structure of a Cu_2O_3 plane reduces to the $2N_y$ degenerate structure of one isolated Cu_2O_5 ladder, with two holes per ladder. As for the CuO_2 plane [16], the simplest approximation consists in retaining only the coupling between the $d_{x^2-y^2}$ orbital of the copper and the p_x or p_y orbitals of the oxygen atoms which have the strongest overlap (Fig. 1b). The band structure is made of seven branches. The eigen states and energy levels are given by:

$$\begin{aligned} \langle \mathbf{r}|\Psi_{n,k}\rangle = \sum_{l=1}^{N_y} \{ \mathrm{e}^{ikla} (a_{n,k}\ \chi(\mathbf{r}-\mathbf{r_l}^{(1)}) + b_{n,k}\ \chi(\mathbf{r}-\mathbf{r_l}^{(2)}) \\ + c_{n,k}\ \Phi_x(\mathbf{r}-\mathbf{r_l}^{(3)}) + d_{n,k}\ \Phi_x(\mathbf{r}-\mathbf{r_l}^{(4)}) \\ + e_{n,k}\ \Phi_x(\mathbf{r}-\mathbf{r_l}^{(5)}) + f_{n,k}\ \Phi_y(\mathbf{r}-\mathbf{r_l}^{(6)}) \\ + g_{n,k}\ \Phi_y(\mathbf{r}-\mathbf{r_l}^{(7)}))\} \end{aligned} \tag{1a}$$

and

see equation (1b) above

with $\chi\ (\mathbf{r}) = \langle \mathbf{r}|d_{x^2-y^2}\rangle, \phi_x\ (\mathbf{r}) = \langle \mathbf{r}|p_x\rangle$ and $\phi_y \mathbf{r} = \langle \mathbf{r}|p_y\rangle$. The vectors $\mathbf{r}_l^\alpha$ locates the atom indexed α, with $\alpha = 1, ..., 7$ (Fig. 1b), of the lth cell. The normalization of $|\psi_{n,k}\rangle$ involves: $|a_{n,k}|^2 + |b_{n,k}|^2 + |c_{n,k}|^2 + |d_{n,k}|^2 + |e_{n,k}|^2 + |f_{n,k}|^2 + |g_{n,k}|^2 = 1$. ε_p and ε_d are respectively the atomic level of the oxygen and copper atoms, $\gamma_x = \langle p_x|H_0|d_{x^2-y^2}\rangle$ is the transfer integral between the copper and oxygen atoms indexed by $\alpha = 1$ and $\alpha = 4$ respectively, $\pm\gamma'_x$ the one between the copper and the oxygen atoms $\alpha = 3, 5$

and $\gamma_y = \langle p_y|H_0|d_{x^2-y^2}\rangle$ between the oxygen sites $\alpha = 6, 7$ and the copper sites $\alpha = 1, 2$ respectively. H_0 is the non interacting Hamiltonian. The diagonalization of (1) is straightforward. One gets:

$$\varepsilon_k = \varepsilon_p \text{ for } \begin{cases} a_k = b_k = 0 \\ -\gamma'_x c_k + \gamma_x d_k + \gamma_y(1 - \mathrm{e}^{-ika}) f_k = 0 \\ -\gamma_x d_k + \gamma'_x e_k + \gamma_y(1 - \mathrm{e}^{-ika}) g_k = 0 \end{cases} \tag{2a}$$

and

$$\varepsilon^{\pm}_{1,k} = \frac{\varepsilon_d + \varepsilon_p}{2} \pm \sqrt{\left(\frac{\varepsilon_d - \varepsilon_p}{2}\right)^2 + \gamma'^2_x + 2\gamma^2_y(1 - \cos ka)}$$

for $a_k = b_k = d_k = 0$,

$$\varepsilon^{\pm}_{2,k} = \frac{\varepsilon_d + \varepsilon_p}{2} \pm \sqrt{\left(\frac{\varepsilon_d - \varepsilon_p}{2}\right)^2 + 2\gamma^2_x + \gamma'^2_x + 2\gamma^2_y(1 - \cos ka)}$$

for $a_k = -b_k = \frac{\varepsilon_p - \varepsilon^{\pm}_{2,k}}{2\gamma_x} d_k$,
and

$$c_k = (-1)^n e_k = \frac{-\gamma'_x}{\varepsilon_p - \varepsilon^{\pm}_{n,k}} a_k,$$
$$f_k = (-1)^{n+1} g_k = \frac{\gamma_y(1 - \mathrm{e}^{ika})}{\varepsilon_p - \varepsilon^{\pm}_{n,k}} a_k. \tag{2b}$$

The three bands reducing to the oxygen level ($\varepsilon_k = \varepsilon_p$) have a vanishing weight on the copper atoms. As in the CuO_2 plane, the inclusion of a small coupling between the nearest neighbor oxygen atoms would simply replace this discrete level by a very tight band, well below the Fermi level. This latter is crossed by the two antibonding bands ($\varepsilon^+_{1,k}$) and ($\varepsilon^+_{2,k}$) expressed in (2b). To clarify their physical meaning, let us consider the limit $|\varepsilon_d - \varepsilon_p| \gg \gamma_{x,y}$:

$$\varepsilon^+_{1,k} = \varepsilon_0 + t_x - 2t_y \cos ka$$
$$\varepsilon^+_{2,k} = \varepsilon_0 - t_x - 2t_y \cos ka \tag{3}$$

with $\varepsilon_0 = \max(\varepsilon_d, \varepsilon_p) + \frac{\gamma'^2_x + \gamma_x + 2\gamma_y}{|\varepsilon_p - \varepsilon_p|}$, and $t_{x,y} = \frac{\gamma^2_{x,y}}{|\varepsilon_p - \varepsilon_p|}$. Therefore ($\varepsilon^+_{1,k}$) and ($\varepsilon^+_{2,k}$) are respectively the antibonding and bonding bands resulting from the coupling between the antibonding sub-bands ($\varepsilon^+_k = \varepsilon_0 + 2t_y \cos ka$) of the two Cu-O chains. In the ideal case, $t_x = t_y = t$. Then, the two bands structure is symmetric with respect to ε_0, that coincides with the Fermi level in the undoped material. Especially, the coupling between the two 1D Cu-O chains does not lead to a loss of nesting of the Fermi surface: indeed, for $t_x = t_y$, the *same vector* $q = 2\pi/3a$ connects the two opposite sides $\pm k_{nF}$ of the Fermi surface for each one of the two bands $n = 1$ and $n = 2$, whose respective fillings are 1/3 ($k_{1F} = \pi/3$) and 2/3 ($k_{2F} = 2\pi/3$). Thus, the whole Fermi surface is nested by q for which we expect strong Spin Density Wave (SDW) correlations that could explain the gap observed in the susceptibility and transport measurements (Sect. 3). For $t_x \neq t_y$, or upon doping, the nesting of each band is no longer realized by the same vector. Therefore, we expect this gap to depend strongly on the ratio t_y/t_x and on the doping rate. Contrary to the CuO_2 plane, the Fermi level is far from the van Hove singularities ($\varepsilon = \varepsilon_0 \pm t$) and ($\varepsilon = \varepsilon_0 \pm 3t$), lying at the top and the bottom of each bands: the oxydation degree needed to reach the closest singularity ($\varepsilon = \varepsilon_0 - t$) by hole doping is $Cu^{2.5}$. Thus, the two-leg ladder compounds, in this model, are much less favourable to the high T_c superconductivity than the 2D cuprates. We have excluded in this paper the more complex case of $(Sr, Ca)_{14}Cu_{24}O_{41}$ [33], that contains 7 ladders planes Cu_2O_3 and 10 planes of CuO_2 chains [34], where a superconducting transition is observed around 12 K under high pressure [35], since this latter is attributed to the chains [36].

2.2 The three-leg ladder

The ladder plane of $Sr_2Cu_3O_5$ is shown in Figure 1a: each ladder consists of three Cu-O chains coupled by "double rungs". The unit cell (Cu_6O_{10}) contains two ladders along the **b** axis that, with the same approximation as in 2.1, we consider as decoupled. The electronic band structure of one isolated ladder Cu_3O_7 contains ten branches, four of them reducing to the oxygen atomic level. The other six bands are divided in three bonding and three antibonding bands. These result respectively from the coupling between the bonding (antibonding) sub-bands of the three Cu-O chains. In $Sr_2Cu_3O_5$, with one hole per copper site, the Fermi level lies in the antibonding states. For $|\varepsilon_d - \varepsilon_p| \gg \gamma_{x,y}$, one gets:

$$\varepsilon^+_{1,k} = \varepsilon_0 + \sqrt{2}t_x - 2t_y \cos ka$$
$$\varepsilon^+_{2,k} = \varepsilon_0 - 2t_y \cos ka$$
$$\varepsilon^+_{3,k} = \varepsilon_0 - \sqrt{2}t_x - 2t_y \cos ka. \tag{4}$$

This expression can be generalized by ($\varepsilon^{(d)}_{n,k} = \varepsilon_0 - 2t \cos \frac{n\pi}{d+1} - 2t \cos ka$), with d the number of Cu-O chains, which gives the usual bidimensional relation dispersion ($\varepsilon_k = \varepsilon_0 - 2t \cos k_x a - 2t \cos k_y a$) when d goes to infinity. As for the two-leg ladder, the antibonding part of the band structure is symetric with respect to ε_0, and the Fermi level ε_F is $\varepsilon_F = \varepsilon_0$. As shown in Figure 2, the nesting vector is $q_1 = \pi/2a$ for ($\varepsilon^+_{1,k}$) and ($\varepsilon^+_{3,k}$), whose respective fillings are 1/4 and 3/4, and $q_1 = \pi/a$ for ($\varepsilon^+_{2,k}$) which is half filled. The metallic state is therefore unstable against a SDW state (for sufficient 3D couplings), characterized by the two vectors q_1 and $q_2 = 2q_1$. Note that the presence of this second harmonic is not simply due to the self consistency, but essentially to the band ($\varepsilon^+_{2,k}$) that crosses the Fermi level for $k_F = \pm\pi/2a$. As we will see in the next section, the fact that the Fermi Surface is nested by two different vectors will lead to a strong reduction of the gap

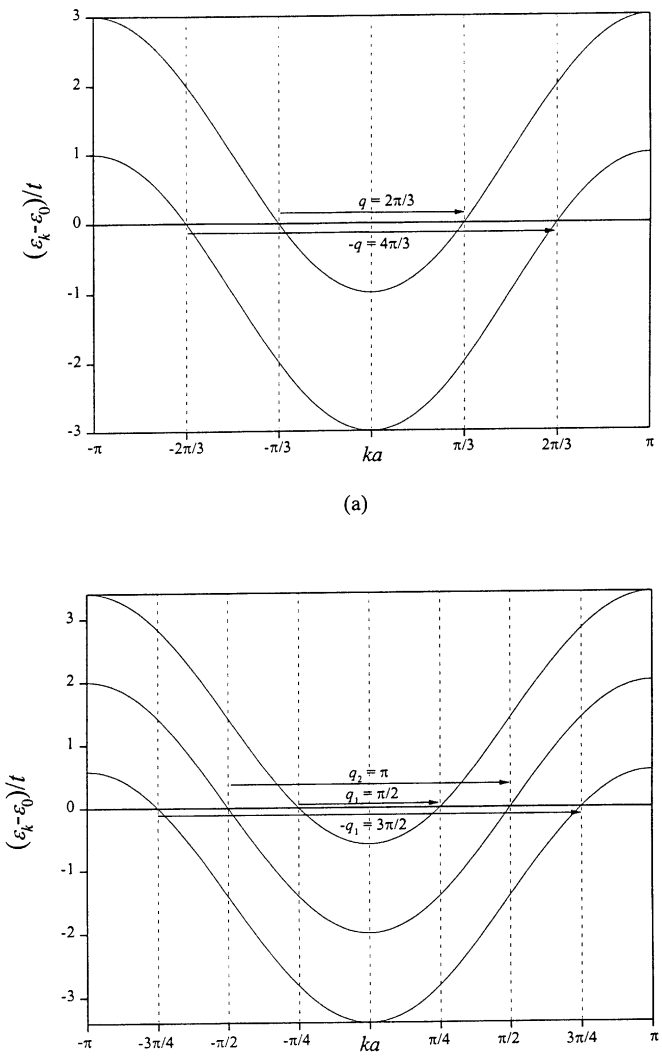

Fig. 2. Band structure of the ladder for $n = 2$ (a) and $n = 3$ (b). The arrows represent the nesting vectors in the undoped material.

in the elementary excitations even if a long range order is stable. Doping or a variation of the ratio t_y/t_x will also reduce the gap. As in the two-leg ladder, the Fermi level is rather far from the van Hove singularities in the undoped material since the closest singularity corresponds to $Cu^{2.27+}$. Moreover, due to the interchain coupling that lowers the degeneracy, the amplitude of each 1D singularity is divided by 3 with respect to the isolated chain.

3 Magnetic structure of the two-leg and three-leg ladder

Due to the nesting properties of the Fermi surface for both the two-leg and three-leg ladders, the inclusion of an arbitrarily weak *on site* repulsion leads at mean field level and $T = 0$ K, to a SDW order of vector $2k_F$ which lowers the coulombic energy for vanishing kinetic cost. Beyond mean field, the long range order is reduced by the Goldstone modes ($\omega_q \to 0$) associated with the broken symmetry. In the undoped material, these reduce to the spin rotation modes, corresponding to the spin independence of the interaction Hamiltonian in the absence of external (or local) magnetic field. The phasons have for their part a finite energy for $q \to 0$, since the magnetic order is commensurate with the lattice, as for the CuO_2 plane at half-filling.

For $d \leq 2$, the thermal fluctuations are sufficient to destabilize the long range order at finite temperature [37], and for $d = 1$, the long range order is destroyed even at $T = 0$ K by the Goldstone modes; in this case the system is characterized by a slow algebraic decay of the spin correlations in real space (*quasi long range order*) [38], whereas, in the presence of a magnetic potential, the spin rotation modes have a gap and the SDW is stable at $T = 0$ K, as for $d = 2$. But in fact, in the real material, the existence of small 3D couplings allows for the existence of an ordered phase at finite temperature. This is observed in the 2D cuprates for which a 3D antiferromagnetic state is stable with, for instance, a Neel temperature $T_N = 250$ K in La_2CuO_4. For $T > T_N$, the three-dimensional order is replaced by strong bidimensional spin fluctuations inside each CuO_2 plane [39]. Therefore, a bidimensional mean field discussion is qualitatively valid, although the calculated critical temperature, corresponding to the annulation of the moments, is larger than the experimental T_N, that corresponds to their disordering [19]. In this section we will apply the same description to the ladder materials since many of their electronics properties (transport and magnetism) seem to be determined by the physics of the 1D ladder [26,28–30].

3.1 The two-leg ladder

Close to the Fermi level, the band structure of the two-leg ladder can be described, for $|\varepsilon_d - \varepsilon_p| \gg \gamma_{x,y}$, by the effective Hamiltonian:

$$H_0 = \sum_{\substack{k,\sigma \\ n=1,\ 2}} \varepsilon_{n,k}\ a^+_{n,k,\sigma}\ a_{n,k,\sigma}$$

$$\varepsilon_{\frac{1}{2},k} = \varepsilon_0 \pm t - 2t\cos ka$$

$$a^+_{\frac{1}{2},k,\sigma} = \frac{1}{\sqrt{2N_y}} \sum_{l=1}^{N_y} \mathrm{e}^{ikla}(c^+_{l,1,\sigma} \pm c^+_{l,2,\sigma}) \qquad (5)$$

where $c^+_{l,1,\sigma}(c^+_{l,2,\sigma})$ is the electron creation operator on the 1st (2nd) copper site of the 1th rung. $a^+_{1,k,\sigma}(a^+_{2,k,\sigma})$ creates an electron in the antibonding (bonding) state arising from the coupling between the two Cu-O chains, t is the transfer integral between nearest neighbor copper sites mediated by the intercalated oxygen atom. Adding the Hubbard *on site* repulsion, expressed in the k space, we get:

$$H = H_0 + H_1$$

$$H_1 = \frac{U}{N_y} \sum_{\substack{k,k',q \\ n=1,\ 2}} a^+_{n,k,\uparrow} a_{n,k+q,\uparrow} a^+_{n,k'-q,\downarrow} a_{n,k',\downarrow}. \qquad (6)$$

For a sinusoidal SDW of vector $\pm q_0 = 2\pi/3a$, the linearized Hamiltonian is:

$$H_{MF} = \sum_{k,n,\sigma} E_{n,k}\ a^+_{n,k,\sigma}\ a_{n,k,\sigma} - U\frac{m}{2}\sum_{n,k,\sigma}\sigma(a^+_{n,k-q_0,\sigma}\ a_{n,k,\sigma} + h.c.) - 2UN_y(\frac{\rho^2}{4} - \frac{m^2}{2}) \quad (7)$$

where $E_{n,k} = \varepsilon_{n,k} + U\frac{\rho}{2}, \rho = \langle c^+_{l,i,\uparrow}c_{l,i,\uparrow}\rangle + \langle c^+_{l,i,\downarrow}c_{l,i,\downarrow}\rangle$, is the electron number per copper atom (with $\rho = 1$ in the undoped material), and $m = \frac{1}{2}\sum_{n,k}\langle a^+_{n,k-q_0,\uparrow}a_{n,k,\uparrow}\rangle = -\sum_{n,k}\langle a^+_{n,k-q_0,\downarrow}a_{n,k,\downarrow}\rangle$ the amplitude of the modulation. The corresponding spin density in the real space can be written: $\rho_{l,i,\sigma} = \langle c^+_{l,i,\sigma}c_{l,i,\sigma}\rangle = \frac{\rho}{2} + \sigma m\cos(\frac{2\pi}{3}l)$ for $i = 1, 2$. In the ordered state, the 1st Brillouin zone is divided by 3. Therefore the exact resolution of (7) reduces to a 3×3 matrix, from which the value of m can be determined by a self-consistent numerical calculation. To get an analytical expression, however, we will use the standard approximation that consists in keeping only the states lying close to the Fermi level, since they bring the main contribution to the SDW. By linearizing the dispersion relations of the two bands close to the Fermi points, we get:

$$E^{\pm}_{1,k} = \varepsilon_0 \pm \sqrt{\left(\frac{Um}{2}\right)^2 + \nu_F^2(|k| - k_{1F})^2} \qquad \text{for } |k| < \frac{\pi}{3a}$$

$$E^{\pm}_{2,k} = \varepsilon_0 \pm \sqrt{\left(\frac{Um}{2}\right)^2 + \nu_F^2(|k| - k_{2F})^2} \qquad \text{for } |k| < \frac{2\pi}{3a} \quad (8)$$

where ν_F is the Fermi velocity, given by $\nu_F = \sqrt{3}\ ta$ for each one of the two bands. The Bragg reflection wavevector $\pm\frac{2\pi}{3a}$ opens a Slater gap $\Delta = Um$ at the Fermi level for the two bands, as the quantum resonance between the Fermi points is induced by the same potential $Um/2$ (Eq. (7)). As a result, the SDW is insulating and a gap in the magnetic excitations is expected for $q \to 0$ at low temperature, as observed in the Curie susceptibility measurements [26,32]. The mean field value of $\Delta(T = 0)$ is obtained by minimizing the total energy. From (7, 8), we get:

$$\int_0^{\frac{\pi}{3a}} \frac{dk}{\sqrt{\frac{\Delta^2}{4} + \nu_F^2k^2}} + \int_0^{\frac{2\pi}{3a}} \frac{dk}{\sqrt{\frac{\Delta^2}{4} + \nu_F^2k^2}} = \frac{4\pi}{Ua}\cdot \quad (9)$$

Assuming that $\Delta \ll \nu_F k_{iF}$, equation (9) gives:

$$\Delta(T = 0) = \frac{4\pi\sqrt{2}\nu_F}{3a}\exp(-\frac{2\pi\nu_F}{Ua})\cdot \quad (10)$$

As the nesting is realized for the two bands Δ has the same exponential behavior as for an isolated chain. With $\nu_F = \sqrt{3}ta$, we get: $\frac{\Delta(0)}{t} \approx 10.26\ \exp(-10.00t/U)$. In La_2CuO_4, it was found in [18] that the experimental value $m_0 \approx 0.4$ corresponds, in the mean field approximation, to $t/U = 0.5$. Such a value is consistent with the basic assumption of itinerant electrons. Due to the quantum fluctuations a larger value of U is actually needed but, as we use here the same approximation, we have kept this ratio for the calculation. We get $\Delta(0)/t \approx 0.44$, leading to $\Delta \approx 440$ K for $t = 1$ eV and $\Delta \approx 220$ K for $t = 0.5$ eV. Such values are in qualitative agreement with the susceptibility measurements performed in $SrCu_2O_3$ ($\Delta \approx 420$ K), but also in $La_2Cu_2O_5$ where the interladder coupling is stronger. In this latter, however, this additional coupling is probably necessary for a correct description of the electronic structure, as suggested by [14].

Our main difficulty is that the gap found in our model should correspond to a magnetic order (with vector q_0) which has not been detected in $SrCu_2O_3$ by the Cu-NMR and μSR measurements, contrary to the $n = 3$ compound $Sr_2Cu_3O_5$ where it is observed for 50–60 K (see Sect. 3.2). To explain this discrepancy, one could argue that the strong 1D fluctuations may destroy the long range order, which would be stable only in $La_2Cu_2O_5$ because of the 3D coupling. The problem is that the magnetic transition is also observed in $Sr_2Cu_3O_5$, where the interladder coupling is expected to be the same as in $SrCu_2O_3$.

As far as $SrCu_2O_3$ is concerned, the results found in an Heisenberg model seem to be in better agreement, at least qualitatively, with the experimental data: the ground state is found to be magnetically disordered, and the gap observed in the uniform susceptibility can be identified as the spin gap corresponding to the triplet collective excitations ($\Delta^{S.G.} \approx J/2$ [9–11]). But, the situation is more complex when we compare the results found in $SrCu_2O_3$ and in $La_2Cu_2O_5$: indeed, while a magnetic ordered phase is detected in $La_2Cu_2O_5$, up to 117 K, the uniform susceptibility $\chi(T)$ shows a remarkable similarity in the two compounds, and was fit in [32] by the same law $\chi(T)\alpha\ T^{-1/2}\exp(-\frac{\Delta}{T})$, where Δ is the spin gap equal to 420 K in $SrCu_2O_3$ and 473 K in $La_2Cu_2O_5$. The existence of such a gap in the magnetic state is quite natural in the case of a SDW, provided the full Fermi surface is nested by the same vector (see Sect. 3.2); but it seems more paradoxical in a Heisenberg model, as the spin rotation modes should contribute to $\chi(T)$ in the ordered phase. To reconcile these results, it was suggested in [14] that, in $La_2Cu_2O_5$, the intermediate value of the ratio $\lambda = J'/J$ (where J and J' are respectively the intraladder and interladder couplings) would place the system close to the quantum transition between the Spin Liquid and the 3D antiferromagnetic state. This would lead to a very small value of $\chi(T = 0)$ in the ordered state, ($\chi(T = 0)$ is exactly equal to zero for the critical ratio λ_c corresponding the quantum transition), and its low temperature behavior would be indistinguishable from an activated one. However, the phenomenological value corresponding to the experimental critical temperature $T_0 = 117$ K is $\lambda = 0.13$ (while $\lambda_c = 0.121$), rather far from the theoretical one, $\lambda' = 0.25$ that places the system well within the A.F. phase. Moreover, assuming that $\lambda = 0.13$, the non neglectable value of T_0 suggests that the staggered

moment, and therefore the susceptibility $\chi(T)$, is quickly increased as soon as $\lambda > \lambda_c$.

Finally, we note that the magnetic solution studied for $La_2Cu_2O_5$ by [14], by introducing in the weak coupling limit the interladder coupling, is very different from the one obtained in this section for the isolated ladder: the authors found the antiferromagnetic solution of vector $[\pi/a, \pi/a, \pi/a]$, as for the 2D cuprates, to be stable for a small finite value of U due to an imperfect nesting of the Fermi surface, instead of $q = 2\pi/3$ along **b** in our calculation. It would therefore be interesting to study the evolution of the nesting vector with respect to the inter ladder coupling.

3.2 The three-leg ladder

Close to the Fermi level, the band structure of the three-leg ladder is described by:

$$H_0 = \sum_{\substack{k,\sigma \\ n=1,\,2,\,3}} \varepsilon_{n,k}\; b^+_{n,k,\sigma} b_{n,k,\sigma}$$

$$\varepsilon_{n,k} = \varepsilon_0 - 2t\cos\frac{n\pi}{4} - 2t\cos ka$$

$$b^+_{n,k,\sigma} = \frac{1}{\sqrt{N_y}}\sum_{l=1}^{N_y}\left\{ \mathrm{e}^{ikla} \times \frac{1}{\sqrt{2}}\sum_{p=1}^{3}\left(\sin\frac{np\pi}{4} c^+_{l,p,\sigma}\right)\right\}. \tag{11}$$

As seen in Section 2, the Fermi surface is nested by two distinct vectors: $q_1 = \frac{\pi}{2}$ for the bands $n = 1$, 3 and $q_2 = 2q_1$ for the band $n = 2$. The magnetic state is therefore characterized by the two components parameter $\chi = (\Delta_1, \Delta_2)$ with $\Delta_i = Um_i$ and $m_i = \frac{1}{2}\sum_{n,k}\langle b^+_{n,k-q_i,\uparrow} b_{n,k,\uparrow}\rangle = -\frac{1}{2}\sum_{n,k}\langle b^+_{n,k-q_i,\downarrow} b_{n,k,\downarrow}\rangle$, which in the real space corresponds to the spin density: $\rho_{l,i,\sigma} = \rho/2 + \sigma m_1 \cos(\pi l/2 + \phi_1) + m_2/2\cos(\pi l + 2\phi_1 + \phi_2)$. In the absence of external magnetic field, the total energy is invariant by translation, so we can choose $\phi_1 = 0$. Moreover, as $m_2/2\cos(\pi l + \phi_2) = m_2/2\cos\phi_2\cos\pi l$, the two parameters m_2 and ϕ_2 reduce to a single one ($m_2/2\cos\phi_2 \to m_2$) and $\rho_{l,i,\sigma}$ is:

$$\rho_{l,i,\sigma} = \frac{\rho}{2} + \sigma\left[m_1\cos\frac{\pi l}{2} + \frac{m_2}{2}\cos\pi l\right]. \tag{12}$$

The pre-factor $m_2/2$ for the second harmonic comes from the fact that $-q_2$ is the same vector as q_2, while both q_1 and $-q_1$ contribute to the first harmonic. The linearized Hubbard Hamiltonian writes:

$$\begin{aligned} H_{MF} = &\sum_{k,n,\sigma} E_{n,k}\; b^+_{n,k,\sigma}\; b_{n,k,\sigma} \\ &- U\frac{\sigma}{2}\sum_{n,k,\sigma}(\Delta_1 b^+_{n,k-q_1,\sigma}\; b_{n,k,\sigma} \\ &+ \Delta_2\; b^+_{n,k-q_2,\sigma}\; b_{n,k,\sigma} + h.c.) \\ &- 2N_y\left(\frac{U\rho^2}{4} - \frac{\Delta_1^2}{2U} - \frac{\Delta_2^2}{4U}\right) \end{aligned} \tag{13}$$

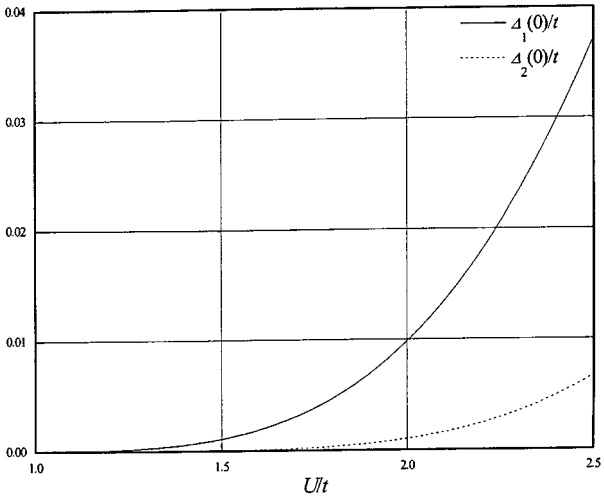

Fig. 3. Variation of the reduced order parameter $(\Delta_1/t, \Delta_2/t)$ *versus* U/t for $T = 0$ K.

with $E_{n,k} = \varepsilon_{n,k} + U\rho/2$ and $\rho = 1$ in the undoped ladder. As previously, we propose a simplified version of the exact resolution of (13), this latter consisting in the diagonalisation of a 4×4 matrix resulting from the modulation of vector $\pi/2a$ of the coulombic potential. For each band, we will consider only the scattering vector connecting the opposite sides of the Fermi surface: q_1 for $n = 1, 3$ and q_2 for $n = 2$. Close to the Fermi level, the one electron energies are given by:

$$E^{\pm}_{n,k} = \varepsilon_0 \pm \sqrt{\left(\frac{\Delta_1}{2}\right)^2 + \nu_{1F}^2(|k| - k_{nF})^2} \qquad \text{for } n = 1,\ 3$$

$$E^{\pm}_{2,k} = \varepsilon_0 \pm \sqrt{\left(\frac{\Delta_2}{2}\right)^2 + \nu_{2F}^2(|k| - k_{2F})^2} \tag{14}$$

with $\nu_{1F} = \sqrt{2}ta$ for and $\nu_{2F} = 2ta$. Contrarily to the two-leg ladder, the gap opened at the Fermi level does not have the same amplitude for every band, since the scattering potential has two distinct values, Δ_1 and Δ_2 (for a given magnetic state) according to the considered band. Using equations (13, 14), the minimization of the total energy leads to:

$$\Delta_1(0) = \pi\sqrt{3}\frac{\nu_{1F}}{a}\exp\left(-\frac{3\pi\nu_{1F}}{Ua}\right) \approx 7.70\; t\; \exp\left(-13.33\frac{t}{U}\right)$$

$$\Delta_2(0) = 2\pi\frac{\nu_{2F}}{a}\exp\left(-\frac{3\pi\nu_{2F}}{Ua}\right) \approx 12.57\; t\; \exp\left(-18.85\frac{t}{U}\right). \tag{15}$$

In equation (15), $\Delta_1(0)$ and $\Delta_2(0)$ differ essentially in the two distinct values ν_{1F} and ν_{2F} of the Fermi velocities present in the exponential factor, the reduction being larger for $\Delta_1(0)$ than for $\Delta_2(0)$. The variations of $\Delta_1(0)$ and $\Delta_2(0)$ with respect to U/t are shown in Figure 3. For $U = 2t$, one gets $\Delta_1(0)/t \approx 9.8 \times 10^{-3}$ and $\Delta_2(0)/t \approx 1.0 \times 10^{-3}$ which leads to $\Delta_1(0) \approx 98$ K and $\Delta_2(0) \approx 10$ K for $t = 1$ eV. As a result, the gap in

the individual excitations, given by Δ_2, has a very small value at $T = 0$, and vanishes at very low temperature, although $\Delta_1(0)$ and the critical temperature of the magnetic transition are of a few tens of Kelvins. An important consequence is that, in the ordered phase, individual excitations are quickly present in the band ($E_{2,k}$) when T is increased from zero, giving rise to a gapless susceptibility

As expressed in equation (15), the expressions of $\Delta_1(0)$ and $\Delta_2(0)$ are independent in the above calculation, because the bands contributing to each one of the two harmonics are distinct. This would lead to two critical temperatures, corresponding to the annulation of each harmonic. Actually, $\Delta_1(0)$ and $\Delta_2(0)$ are linked from equation (13) by the self consistency, and vanish rigorously for an unique temperature T_c. Our simplified calculation, however, shows that there exists two ranges of temperature: $0 < T < T_2$ (with T_2 close to the usual mean field value $\Delta_2(0)/3.52 \cong 3$ K) for which each one of the two harmonics is due to the nesting properties of the Fermi surface, and $T_2 < T < T_c$ (with T_c close to $\Delta_1(0)/3.52$) where the second harmonic $\Delta_2 \approx 0$ since it is only due to the self-consistency. Thus, as soon as $T > T_2$, the gap Δ_2 is much smaller than T and becomes indistinguishable in the Curie susceptibility. Moreover, the exponential behavior, for $T < T_2$, is very difficult to observe experimentally because of the presence of a diverging component in the experimental susceptibility for $T = 0$ K [23]. This latter was attributed by the authors to an impurity phase. Therefore, due to the existence of two nesting vectors, the magnetic ordering observed around 50–60 K in $Sr_2Cu_3O_5$ by the NMR and μSR measurements [28,29] does not coincide with the opening of a gap in the Curie susceptibility, as it is observed in [26]. In the Heisenberg model, the magnetic ordering is consistent qualitatively with the expectation, at mean field level, of an antiferromagnetic state [9]. Beyond mean field the critical temperature strongly depends on the three-dimensional coupling, and the collective modes form an acoustic branch that results in a gapless susceptibility. Therefore, polarized neutrons experiment should be a determining test for the two approaches by determining the vector of the spin modulation.

4 Conclusion

We have studied, in the limit of small *on site* coulombic repulsion, the magnetic instabilities of ideal ladder systems, consisting of n Cu-O chains coupled by Cu-O-Cu rungs, in the cases $n = 2$ and $n = 3$. The aim was to propose an alternative theoretical description of the two-leg and three-leg ladder cuprates [8] in the undoped regime, that have been intensively studied in the opposite limit of the Heisenberg model [9–11,27]. This work is a natural extension of the Fermi liquids studies [16–21], with phonon mediated attraction, that have been proposed to describe the electronic properties of the CuO_2 plane, essentially the antiferromagnetism and the high Tc superconductivity. It does not apply to the more complex ladder compound $(Sr, Ca)_{14}Cu_{24}O_{41}$ [33,34], where a superconducting transition around 12 K under high pressure is attributed to the CuO_2 chains, also present in the structure [35,36].

In the undoped system, the (quasi one-dimensional) Fermi surface is found to be nested by different vectors according to the number of legs: $q = 2\pi/3$ for $n = 2$ and, for $n = 3$, two distinct vectors, $q_1 = \pi/2$ and $q_2 = \pi$, connect distinct parts of the Fermi surface. This leads in both cases to commensurate SDW correlations with these same vectors, contrasting with the prediction of AF correlations for $n = 3$ but not for $n = 2$ in the Heisenberg model. Such a difference suggests that polarized neutrons measurements would provide an essential test for the theory.

The better agreement with the existing experimental results is found for $n = 3$. Indeed the existence, in our model, of the two distinct nesting vectors q_1 and q_2 leads to a magnetic gap with two components (respectively Δ_1 and Δ_2), lying in distinct electronic bands. At $T = 0$ K, Δ_1 and Δ_2 depending exponentially of the Fermi velocities in their electronic bands, we found $\Delta_2(T = 0\text{ K}) \approx 10$ K, while $\Delta_1(T = 0\text{ K})$ is in a range of 100–400 K, for values of our physical parameters consistent with our itinerant electron model ($U/t = 2{-}2.5$). This could explain the observation, in $Sr_2Cu_3O_5$, of a magnetic ordering at 50–60 K by the NMR and μSr measurements [28,29], while no gap is detected in the uniform magnetic susceptibility: indeed, due to its small value at $T = 0$ K, Δ_2 is quickly decreased at finite temperature, allowing for the existence of individual excitations although the SDW is still stable. Therefore, our results constitute an alternative to the ones obtained in the Heisenberg model, according to which the magnetic state is antiferromagnetic, the contribution to the low temperature susceptibility coming from the Goldstone modes. Thus, as a magnetic order is well established in $Sr_2Cu_3O_5$, the polarized neutron measurements should be of crucial interest to determine the accurate solution.

The comparison is less convincing for $n = 2$: we could explain, by the presence of a single nesting vector in the undoped ladder, the gap observed in the uniform susceptibility for $SrCu_2O_3$ [26], and found correct values of its amplitude for moderate on site repulsion. But the expected SDW order has only been detected experimentally in the specific case of $La_2Cu_2O_5$ [31], for which the interladder coupling is stronger, and which therefore does not constitute the best test for our model. In our model, the gap structure observed in $\chi(T)$ should be due to SDW correlations observable in NMR (and neutrons) measurements. However, we would like to emphasize that the comparison of the experimental results for $SrCu_2O_3$ and $La_2Cu_2O_5$ is peculiarly intriguing: indeed, the uniform susceptibility shows a remarkable similarity for the two compounds (with an estimated activation energy of 420 K and 473 K respectively [32]), while a magnetic order is detected by μSR and NMR measurements for $La_2Cu_2O_5$ only, with a critical temperature of 117 K. To reconcile these features, [14] have studied in a Heisenberg model the effect of the interladder coupling, and suggested that $La_2Cu_2O_5$ could be close to a Spin Liquid/AF transition, corresponding to an inter ladder coupling $J'_c \approx 0.121J$. However, the value

of 117 K for the critical temperature requires an interladder coupling $J' \approx 0.13J$, much lower than the theoretical value ($J'/J = 0.25$) which places the system well within the A.F. phase. Therefore the fully consistent description of the $n = 2$ compound is not yet well established.

Finally, for $n = 2$ and $n = 3$, we have found that the 1D singularity is far from the Fermi level of the undoped material. Therefore, a high T_c superconductiviting phase in these systems is probably difficult to obtain since it requires a large doping rate.

References

1. J. Rossat-Mignod, L.P. Regnault, C. Vettier, P. Burlet, J.Y. Henry, G. Lapertot, Physica B **169**, 58 (1991); P. Bourges, Y. Sidis, L. Regnault, B. Hennion, R. Villeneuve, G. Collin, C. Vettier, J.Y. Henry, J.F. Marucco, J. Phys. Chem. Solids **56**, 1937 (1995).
2. K.A. Chao, J. Spalek, A.M. Oles, J. Phys. C **10**, L271 (1977).
3. F.C. Zhang, C. Gros, T.M. Rice, H. Shiba, Supercond. Sc. Technol. **1**, 36 (1988).
4. M.K. Crawford, M.N. Kunchur, W.E. Farneth, E.M. Mc. Carron III, S.J. Poon, Phys. Rev. B **41**, 282 (1990); J.P. Frank, S. Harker, J.H. Brewer, Phys. Rev. Lett. **71**, 915 (1993); Q. Xiong, J.W. Chu, Y.Y. Sun, S. Bud'ko, P.H. Hor, C.W. Chu, Phys. Rev. B **46**, 581 (1992).
5. A. Bianconi, N.L. Saini, A. Lanzara, M. Missori, T. Rosstti, H. Oyanagi, H. Yamaguchi, K. Oka, T. Ito, Phys. Rev. Lett. **76**, 3412 (1996).
6. J.M. Tranquada, J.D. Axe, N. Ichikawa, A.R. Moodenbaugh, Y. Nakamura, S. Uchida, Phys. Rev. Lett. **78**, 338 (1997).
7. For a review, see R.C. Dynes, Solid State Commun. **92**, 53 (1994); J.R. Schrieffer, *ibid.* **92**, 129 (1994).
8. Z. Hiroi, M. Azuma, M. Takano, Y. Bando, J. Solid State Chem. **95**, 230 (1991).
9. S. Gopalan, T.M. Rice, M. Sigrist, Phys. Rev. B **49**, 8901 (1994).
10. E. Dagotto, J. Riera, D.J. Scalapino, Phys. Rev. B **45**, 5744 (1992).
11. S.R. White, R.M. Noack, D.J. Scalapino, Phys. Rev. Lett. **73**, 886 (1994).
12. C. Haywark, D. Poilblanc, R.M. Noack, D.J. Scalapino, W. Hankee, Phys. Rev. Lett. **75**, 926 (1995).
13. Ph. Germain, M. Laguës, Alloys and Compounds **251**, 222 (1997); E-MRS 1996 Spring meeting, Strasbourg, France, 4-7 june 1996).
14. B. Norman, T.M. Rice, Phys. Rev. B **54**, 7180 (1996); Physica C **282**, 1113 (1997).
15. N. Nücker, J. Fink, B. Renker, D. Ewert, C. Politis, P.J.W. Weijs, J.C. Fuggle, Z. Phys. **67**, 9 (1987); N. Nücker, Springer Series in Solid State Sciences **106** (Heidelberg 1992).
16. J. Labbe, J. Bok, Europhys. Lett. **3**, 1225 (1987).
17. T. Hocquet, J.P. Jardin, Ph. Germain, J. Labbe, Phys. Rev. B **52**, 10330 (1995); Ph. Germain, Ph.D. thesis, University of Paris XI, 1995.
18. R. Combescot, X. Leyronas, Phys. Rev. Lett. **75**, 3732 (1995).
19. T. Hocquet, J.P. Jardin, Ph. Germain, J. Labbe, J. Phys. I France **4**, 423 (1994).
20. T. Hocquet, J.P. Jardin, Ph. Germain, J. Labbe, J. Phys. I France **5**, 517 (1995).
21. S. Charfi-Kaddour, R.J. Tarento, M. Heritier, J. Phys. I France **2**, 1853 (1992); S. Charfi-Kaddour, Ph.D. thesis, University of Paris XI, 1992.
22. P.B. Littlewood, J. Zaanen, G. Aeppli, H. Monien, Phys. Rev. B **48**, 487 (1993).
23. A.V. Chubukov, D. Pines, B.P. Stojkovic, J. Phys.-Cond. **8**, 10017 (1996) (contains many references of the previous works).
24. C.C. Tsuei, C.C. Chi, D.M. Newns, P.C. Pattnaik, Daumling, Phys. Rev. Lett. **69**, 2134 (1992).
25. C. Castellani, C. Di Castro, W. Metzner, Phys. Rev. Lett. **72**, 316 (1994); M. Grilli, C. Castellani, Phys. Rev. B **50**, 16880 (1994).
26. M. Azuma, Z. Hiroi, M. Takano, K. Ishida, Y. Kitaoka, Phys. Rev. Lett. **73**, 3463 (1994).
27. M. Troyer, H. Tsunetsugu, D. Warts, Phys. Rev. B **50**, 13515 (1994).
28. K. Ishida, Y. Kitaoka, Y. Tokunaga, S. Matsumoto, K. Asayama, M. Azuma, Z. Hiroi, M. Takano, J. Phys. Soc. Jpn **63**, 3222 (1994).
29. K. Kojima, A. Keren, G.M. Luke, B. Nashuia,W.D. Wu, Y.J. Uemura, M. Azuma, T. Takano, Phys. Rev. Lett. **74**, 2812 (1995).
30. K. Ishida, Y. Kitaoka, K. Asayama, M. Azuma, Z. Hiroi, M. Takano, J. Phys. Soc. Jpn **63**, 3222 (1994).
31. S. Matsumoto, Y. Kitaoka, K. Ishida, K. Asayama, Z. Iroi, N. Kobayashi, M. Takano, Phys. Rev. B **53**, R11942 (1996).
32. Z. Hiroi, M. Takano, Nature **377**, 41 (1995).
33. T. Siegrist, L.F. Scemeyer, S.A. Sunshine, J.V. Waszak, Mat. Res. Bull. **88**, 1429 (1988).
34. Mc Carron, M.A. Subramanian, J.C. Calabrese, R.L. Harlow Waszak, Mat. Res. Bull. **88**, 1355 (1988).
35. M. Uehara, T. Nagata, J. Akimitsu, H. Takahashi, N. Mori, K. Kiroshita, J. Phys. Soc. Jpn **65**, 2764 (1996).
36. S.A. Carter, B. Battlog, R.J. Cava, J.J. Krajewski, W.F. Peck, T.M. Rice. Phys. Rev. Lett. **77** 1378 (1996);
37. N.D Mermin, H. Wagner, Phys. Rev. Lett. **17**, 1133 (1966).
38. D. Jerome, H.J. Shultz, Adv. Phys. **31**, 299 (1982).
39. Y. Endoh, K. Yamada, R.J. Birgeneau, D.R. Gabbe, H.P. Jenssen, M.A. Kastner, C.J. Peters, P.J. Picone, T.R. Thurston, J.M. Tranquada, G. Shirane, Y. Hidak, M. Oda, Y. Enomoto, M. Suzuki, T. Murakami, Phys. Rev. B **37**, 7443 (1988).